CATALYTIC ACTIVITY OF VANADIUM OXIDE DOPED WITH PALLADIUM NANOPARTICLES ON OXIDATION OF 5-HYDROXYMETHYLFURFURAL

Settakorn Upasen[1,2], Patiparn Boonruam[1,2], Joongjai Panpranot[3], Soipatta Soisuwan[1,2*], and Piyasan Praserthdam[3]

[1]Department of Chemical Engineering, Faculty of Engineering, Burapha University, Chonburi, Thailand
[2]Research Unit of Developing Technology and Innovation of Alternative Energy for Industries, Burapha University, Chonburi, Thailand, e-mail: soipatta@eng.buu.ac.th
[3]Center of Excellence in Catalysis and Catalytic Reaction Engineering, Department of Chemical Engineering, Faculty of Engineering, Chulalongkorn University, Bangkok, Thailand

Abstract

2,5-Furan dicarboxylic acid (FDCA) is a bio-based chemical used as a feedstock for a wide range of industrial applications - particularly the bioplastic industries. It is derived from 5-hydroxymethylfurfural (HMF) through a reaction of oxidation using either homogeneous or heterogeneous catalysts. According to the advantages of heterogeneous catalysts, this research aims to seek a novel catalyst type with high selectivity and high activity. We performed an investigation of the synergic effect of palladium nanoparticles and V_2O_5 catalysts on catalytic oxidation of HMF and physicochemical properties. A commercial vanadium oxide powder (V_2O_5) was doped with 1 wt.% palladium nanoparticles (Pd NPs). The Pd NPs were prepared by the colloid-chemical reduction method. Two different synthesis processes were performed base on the consequence of the combination of colloid-chemical reduction and immobilization steps, herein stepwise (ST) and simultaneous (SI) process. For the ST process, Pd NPs were reduced and then immobilized on V_2O_5 powder. During the SI process, the reduction and immobilization steps took place simultaneously. Physical and chemical properties of a prepared catalyst such as morphology, particle size distribution, and chemical structure and composition were characterized using various techniques, e.g. TEM, BET, X-ray diffraction, UV-vis spectrophotometer. It was distinctly found the synergic effect between Pd NPs and V_2O_5 catalysts on the surface catalytic activity of HMF oxidation and catalytic selectivity. The Pd NPs incorporated catalysts (ST and SI processes) gave catalytic activity at 63%, which are 2-fold in catalytic activity in comparison with bare V_2O_5 catalysts as well as they were selective to FDCA up to 19-24%. The step of catalyst preparation slightly influenced on catalytic activity and yield of FDCA; however, it did alter particle size distribution of Pd NPs and surface characteristics.

Keywords: FDCA derivatives, Heterogeneous catalyst, HMF, Oxidation, Pd/V_2O_5

Introduction

Sugar derivatives, for instance, glucose, sucrose, and fructose, can be converted into valuable chemicals, bioplastics monomers, fine chemicals, and medicines [1]. Regarding the U.S. Department of Energy (DOE) report [2] identified that 2,5-furan dicarboxylic acid (FDCA) is one of the bio-based chemicals included in the twelve essential building chemical blocks. The potential of FDCA biochemicals is the replacing terephthalic acid (TPA) feedstock-a petrochemical product used in the polymer industries, specifically for polyethylene terephthalate (PET) production. As an example, Avantium company uses FDCA to produce poly (ethylene

2,5-furandicarboxylate) (PEF), which is a facile degradable polymer as well as evading bioaccumulation [3], whereas thermal stabilities of PEF and PET are comparable. In the previous year, hence, the market margin for the FDCA reported approximately US$ 300 million, and its compound annual growth rate (CAGR) will enlarge of 8.2% in 2025 [4].

In the route of FDCA production, which derived from an oxidation process of 5-hydroxymethyl-2-furfural (HMF), there are other valuable bio-based chemicals such as 5-hydroxymethyl-2-furancarboxylic acid (HMFCA), 2,5-diformylfuran (DFF), 5-formyl-2-furancarboxylic acid (FFCA) and consecutive reaction network is generally shown elsewhere [5]. The first step can undergo two routes, e.g. HMF to HMFCA (oxidation) either or HMF to DFF (oxidation and dehydration). Subsequently, oxidation and consecutive dehydration or only oxidation can occur to change HMFCA to FFCA or DFF to FFCA, respectively. The final series of the oxidation reaction is to transform FFCA to FDCA.
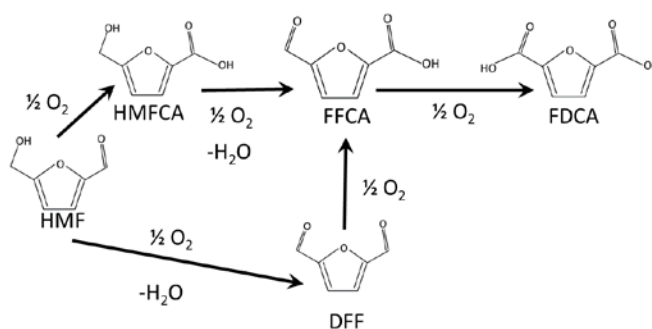

Figure 1. General reaction network of HMF oxidation [5]

The production of FDCA via oxidation of bio-based raw materials, e.g. HMF, employs either homogeneous or heterogeneous catalysts. Several researchers reported the potential of many homogeneous catalysts such as $KMnO_4$, $K_2Cr_2O_7$, $Co(OAC)_2/Zn(OAc)_2/Br^-$ and metal/bromide salts. They were very active to 90% conversion and gave a high yield of FDCA production under different conditions. However, the methodology of homogeneous processes results in inorganic waste and a cumbersome process of separation. Recent development pays attention to the heterogeneous catalytic process. The standard heterogeneous catalysts generally used noble metals loaded over several supporting materials such as Au/TiO_2 [6], $Pt/A_{12}O_3$ [7], Pd/C [8], and Ru/C [9]. These noble metals are well-known since the catalysts were selective excellently to oxidation with molecular oxygen and gave an excellent yield of FDCA production. For example, Zou Bin and co-workers [8] transformed HMF directly into FDCA over Pd/base-modified Activated Carbon catalyst in the water at 373 K for 24 hours resulting in complete conversion of HMF and 82.4% FDCA yield. Tianqi Gao et al. [5] explored that mechanism oxidation reaction of HMF undergoes different pathways, which allows a competition of HMFCA and DFF production. The HMF molecule was selectively oxidized either at the hydroxymethyl group (R-OH) or at aldehyde group (R=O), where located at the second and fifth position at the furan ring, respectively. In the attendance of a strong base, aldehyde groups in HMF and DFF molecules undergo Cannizzaro reaction readily [10], which changes two aldehyde groups to one carboxyl group and one hydroxyl group and lowers the production of FDCA. Several reports have studied selective oxidation of HMF, especially selectivity to DFF intermediate, using various heterogeneous catalytic systems include

vanadium oxide (V_2O_5) [11, 12]. The HMF oxidation to DFF with the surface lattice oxygen atoms on the VOx domains, leading to the reduction of V^{5+} to V^{4+}, such process is known as the Mars–van *Krevelene* redox mechanism. An amount of 85 % DFF yield (93 % selectivity at 91 % conversion) was reported by Moreau and co-workers [12]. However, the catalytic activity of the synergism of vanadium oxide and a noble metal (i.e. palladium, goal, etc.) is rarely studied.

To address the above issue, we studied the potential of the HMF oxidation reaction using alternative Pd nanoparticles incorporated with V_2O_5 catalysts in this research. The Pd/V_2O_5 catalysts were prepared via two different routes: i) stepwise process (ST) and ii) simultaneous process (SI) and physicochemical properties of the synthetic catalysts were characterized by means of TEM, XRD, UV-Visible spectrophotometry and FT-IR spectroscopy. The effect of parameters of catalyst preparation toward catalytic property and efficiency is examined and discussed.

Experimental

Pd/V_2O_5 Catalysts Preparation

Chemicals

All chemicals used in catalysts development were analytical reagent (AR) grade and purchased from commercial suppliers. No further purification was done before using the chemicals.

Pd Colloid Preparation

Preparation of palladium nanoparticles via colloidal method has been described previously [13]. A typical protocol can be summarized as follows. The polyvinyl alcohol (PVA, average MW= 13000-23000, 87%-89% hydrolyzed) was dissolved in water at 70°C aging at least for 2 hours. [Note: the PVA used as a nanoparticle stabilizing agents - can block part of the active sites by covering the majority of the metal surface and can also manipulate adsorbed reactive species on the metal surface, influencing the activity and the selectivity of Pd catalysts] Then, the solution (2 wt.%) was cooled down to room temperature. A 50 ml of PdCl$_2$.2H$_2$O solution (0.2367 mmol Pd) and 5.83 ml of the prepared PVA solution were added into 250 ml DI water. The solution was well mixed for 3 minutes, and its color displayed homogeneity in a yellow-brown. A reducing agent of 0.03 mM NaBH$_4$ solution was slowly added under severe stirring. The reduction reaction of Pd^{2+} can be written in Equation 1; therefore, the brownish Pd colloid solution was formed. The final pH would be detected, typically between 4 to 5.

$$4PdCl_2(aq) + NaBH_4(aq) + 2H_2O(l) \rightarrow 4Pd(s) + NaBO_2(aq) + 8HCl(aq) \qquad (1)$$

Colloid Immobilization

To dope 1 wt.% Pd nanoparticles into V_2O_5, an amount of 3 g V_2O_5 was added to the Pd colloid solution immediately after the colloid preparation. Then, we slowly added a solution of hydrochloric acid (HCl) to modulate pH to ~2. The use of HCl solution during immobilization of Pd colloid on V_2O_5 particles is to destroy the polyvinyl alcohol stabilizing agent from the surface of the Pd nanoparticles (NPs). The slurry was stirred using an overhead stirrer (800 rpm) with a simple propeller placed at the center of liquid. This immobilization process exposed in the air and kept for 2 hours at room temperature. The slurry was then filtered and thoroughly

washed with water several times. In order to dry the obtained solids samples, we placed them in a vacuum oven at 40°C overnight.

The influence of the catalyst preparation process was studied. There are two categories: i) stepwise process (ST) - Pd colloid was done before immobilizing Pd NPs on V_2O_5 ii) simultaneous process (SI) - Pd colloid and immobilization were done at the same time.

Physical and Chemical Characterization

Transmission electron micrographs of the as-synthesized Pd/V_2O_5, as well as V_2O_5 samples, were obtained using a transmission electron microscope (Phillip-Tecnai20 model). The potential magnitude was set at 100 kV with a resolution of 13,5000x-13,000x. The powder samples were dissolved in 99% ethanol and sonicated for a few minutes to ensure the dispersion of particles on the Cu grid (carbon film 300 mesh).

The X-ray diffraction was performed by using the Bruker D8 Advance X-ray diffractometer with Ni-filtered CuKα radiation (λ = 1.54056 Å). The XRD patterns were recorded over an angular range (2θ) of 20-80 degree with 0.5 sec/step. Fourier transform infrared spectra of synthetic samples were obtained by an attenuated total reflectance Fourier Transform (ATR-FTIR) spectrometer (PerkinElmer-Frontier) with an accumulation of 250 scans at a wavenumber range of 4000-400 cm^{-1} and a resolution of 4 cm^{-1}. UV-Visible spectra of the samples were recorded at 500-700 nm using a UV/visible spectrophotometer, Varian Carry 1E model. To prepare the UV-vis analyzed solution, an amount of ~0.1 mg dried powder Pd/V_2O_5 sample was dissolved in pure ethanol using a sonicator.

Oxidation of HMF into FDCA

All the reaction experiments were carried out using a 100 ml batch reactor. The tube reactor was charged with 3 mmol of HMF, 9 mmol of Na_2CO_3, and 38 mmol of TBHP. The catalyst loading was 0.01 g/ml of which was made up to 30 ml by adding acetonitrile as a solvent. The mixed solution in the tube reactor was placed at a water bath, where was set the reaction temperature at 80°C. All the reactions were carried out for 24 hours without any agitation. The reaction samples were collected and kept at cold ambient.

The furan compounds contained in reaction samples were diluted with a hundredfold tetrahydrofuran (THF) and quantitatively analyzed by HPLC (High Prostar model) equipped with a UV detector. The samples were separated at the wavelength of 280 nm using a reverse-phase C18 column (125 x 4 mm). The carrier phase was composed of acetonitrile and 0.1 wt.% acetic aqueous acid solution at 1.0 ml/min flow rate. The calibration curves of standard materials, HMF and FDCA, was received. The specific calculation was as follows.

$$\text{Conversion of HMF} = \frac{\text{initial moles of HMF - final moles of HMF}}{\text{initial moles of HMF}} \times 100\% \tag{2}$$

$$\text{Yield of FDCA} = \frac{\text{moles of FDCA}}{\text{initial moles of HMF}} \times 100\% \tag{3}$$

$$\text{Selectiviy of FDCA} = \frac{\text{moles of FDCA}}{\text{mole of total products}} \times 100\% \tag{4}$$

Results and Discussion

Morphology Characteristics of Synthetic Pd/V$_2$O$_5$

Morphology analysis of V$_2$O$_5$ sample and reduced V$_2$O$_5$ using 0.1 M NaBH$_4$ in 50 ml was done to comprehend the background before incorporating the Pd NPs. The TEM images of both V$_2$O$_5$ and reduced V$_2$O$_5$ sample does not have a specific shape, a representative TEM image, as shown in Figure1 at the right corner on top. The V$_2$O$_5$ particle size measured by the longest attitude show between 1,128 nm and 1,134 nm. Figure 1 shows the micrographs of Pd/V$_2$O$_5$ samples prepared by stepwise (Figure 1a) and the simultaneous process (Figure 1b). Furthermore, the histogram of its particle size distribution is illustrated in Figure 2. With the colloidal synthesis method, the Pd nanoparticles deposited on the surface layer of V$_2$O$_5$ for both samples enhanced a spherical shape. Table 1 indicates the summary of Pd particle size and particle distribution. The particle size of the sample prepared by the stepwise process (Figure 1a, 2a) revealed approximately 2-fold smaller than the one made by the simultaneous process (Figure 1b, 2b). However, the later process affected a high distribution of Pd particles over the V$_2$O$_5$ surface, probably due to the longer immobilizing time steps. On the one hand, the Pd nanoparticles received by the stepwise process appeared close to each other, leads to aggregate into larger particles.

Table 1. Measurement of Pd Particle Size and Distribution

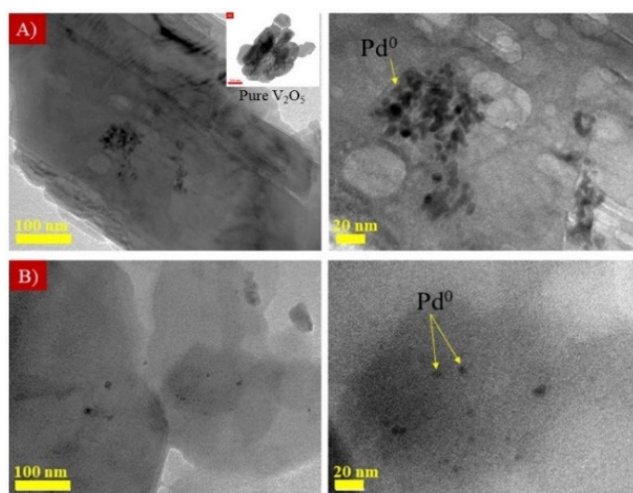| No.	Preparation Method	Pd Content (wt.%)	Particle Size (nm)	Particle Distribution (nm)
1	Stepwise (ST)	1	5 ± 1.93	3.07 - 6.93
2	Simultaneous (SI)	1	11 ± 4.58	6.42 - 15.48

Figure 1. TEM micrographs of synthetic Pd/V$_2$O$_5$ sample obtained by A) stepwise and B) simultaneous [Note: pure V$_2$O$_5$ posed overlap on left-top TEM micrographs]
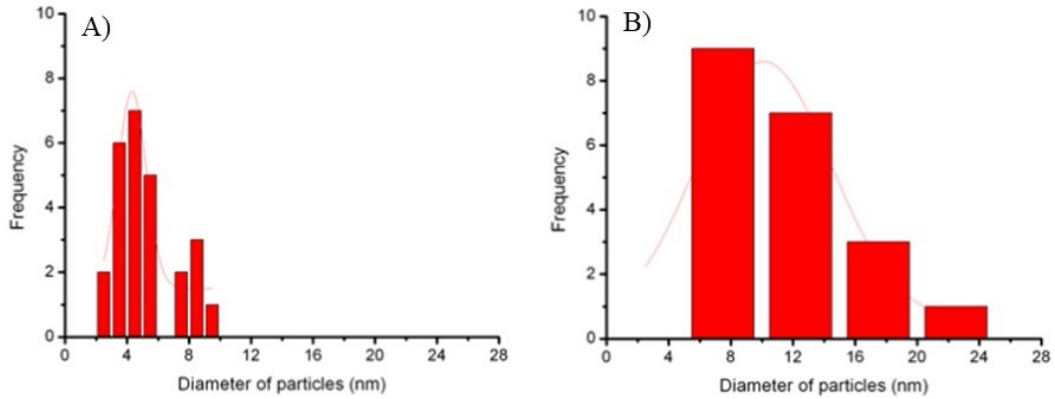
Figure 2. Particle size histogram of synthetic Pd/V_2O_5 sample for A) stepwise synthesis process and B) simultaneous synthesis process

X-ray Diffraction

XRD patterns of V_2O_5 and reduced V_2O_5 sample are displayed in Figure 3. [Note: the reduced V_2O_5 as abbreviated as R-V_2O_5 is a powder sample of V_2O_5 reduced by 0.1 M $NaBH_4$ solution in order to make a comparison of the V^{5+}/V^{4+} reduction effect using $NaBH_4$.] Six strongest peaks located at 20.32°, 21.74°, 26.14°, 31.05°, 32.38°, and 34.35° were observed, corresponding to the characteristic (001), (101), (110), (400), (011) and (310) planes of V_2O_5. These observed peaks are similar to the study of Lianyi Shao et al., which match with the JCDS Card no. 41-1426 [14]. It can be said that both V_2O_5 and reduced V_2O_5 samples exhibited an orthorhombic symmetry group with Pmmn space group (No. 59). The lattice parameters for the both samples were a = 1.5406 Å, b = 1.5444 Å, and c = 1.3902 Å. This observation confirms that the reduction step, which added an amount of 0.1 M $NaBH_4$ into V_2O_5 solution, does not impact on structural modification and chemical composition of V_2O_5 sample.
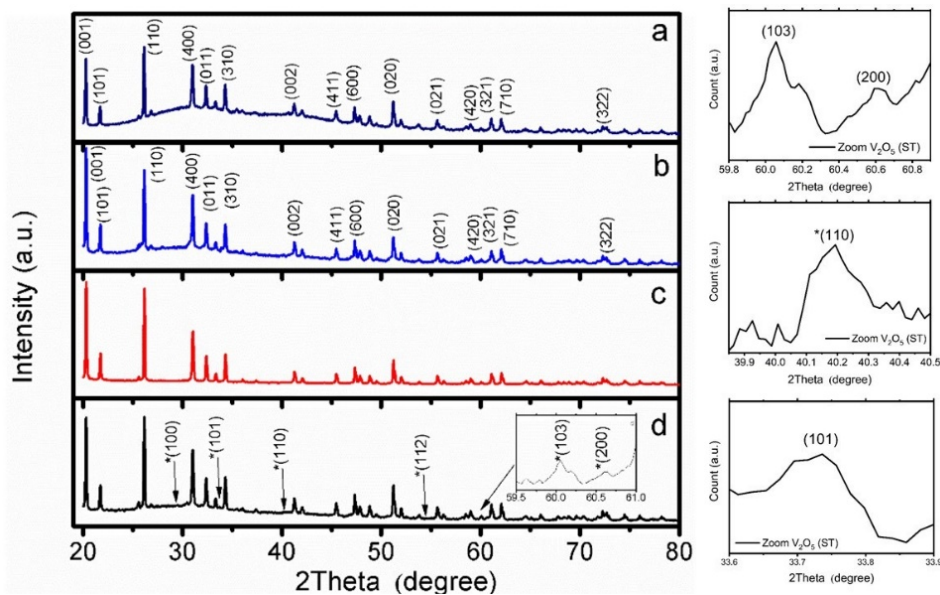

Figure 3. XRD pattern of as-prepared sample: a) V_2O_5, b) R-V_2O_5, c) Pd/V_2O_5 (SI), and d) Pd/V_2O_5 (ST)

In the case of synthetic Pd/V_2O_5 samples received from SI and ST process, XRD patterns illustrate at the red and black spectra, respectively. The Bragg's peaks for both samples did not appear at 40°, 47° and 67°, which indicated a crystalline particle of zero-valent palladium [15] so that Pd^0 nanoparticles immobilized on Pd/V_2O_5 may occur in amorphous form or crystalline Pd^0 nanoparticles occurring is very small and it was undetectable. The traces of crystalline PdO structure were found instead in Pd/V_2O_5 samples received from ST process (Figure 3d). The diffractions peaks were observed at $2\theta = 33.80°$, 40.2°, 60.05° and 60.60° corresponding to the predominant formation of tetragonal phase of PdO, and indexed the characteristic of (100), (112), (103) and (200) planes as illustrated on the right side of Figure 3 [15, 16]. Hence, the stepwise process (ST) leads to an oxidation reaction of Pd^0 nanoparticles to form palladium oxide during the immobilization of Pd^0 nanoparticles to V_2O_5. The steps of palladium oxide formation are shown as the following equation:

$$Pd^{2+} \xrightarrow{BH_4^{2-}} Pd^0 \xrightarrow{V_2O_5(aq)} PdO \tag{5}$$
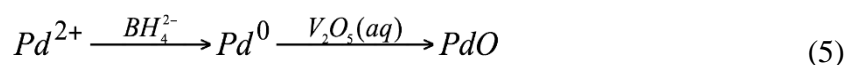
Infrared and UV-Vis Spectroscopy

The structural information of samples is further presented by FTIR and UV-Vis spectra, as shown in Figure 4a and 4b, respectively. The FTIR spectra (Figure 4a) for all the samples observed in the wavenumber 500-2000 cm^{-1}. It is clear that there were three bands in low-frequency range: at ~566 cm^{-1} corresponding to the vibrational characteristic of V-O-V bond, at ~761 cm^{-1} due to the stretching mode of V-O and at ~998 cm^{-1} attributed to the stretching mode of V=O relationships [14, 17, 18]. It notices that the peak located at 1,426 cm^{-1} observed for the reduced V_2O_5 sample can be assigned to symmetric COO^- stretching [17], which represents the carboxyl group of PVA impurity remaining after the preparation process.
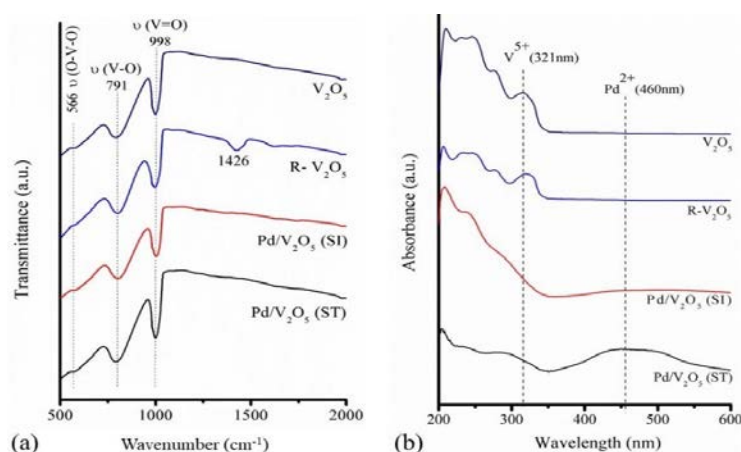

Figure 4. Spectroscopy results of the synthetic samples analyzed by (a) FT-IR (ATR mode) and (b) UV-Visible spectrophotometry

The UV-visible spectra of V_2O_5 and reduced V_2O_5 were shown in Figure 4b. A peak appeared at a wavelength of ~321 nm for both samples regarding the characteristic absorption peak of V(V) ion [19], and it insists that reduction step after adding $NaBH_4$ as a reducing agent does not influence on V_2O_5 chemical structure. These results show in good accordance with the report of XRD that detected similar crystalline structures of an orthorhombic symmetry

group in both V_2O_5 and reduced V_2O_5. In the case of Pd incorporated with V_2O_5 sample, especially the one received from ST process, broadband centered at wavelength 460 nm appeared, it corresponds to the central absorption peak of Pd(II) ion [20] which represents PdO compound in good agreement with PdO crystalline structure detected by XRD.

Catalytic Activity

To examine the catalytic activity for all the catalyst types - V_2O_5, R-V_2O_5, Pd/V_2O_5 (SI), and Pd/V_2O_5 (ST). The oxidation of HMF was performed using TBHP oxidant agent in 30 mL acetonitrile and 9 mmol Na_2CO_3 at 80°C for 24 hrs. The catalyst loading was 0.3 g. Figure 5 (left) illustrates HMF conversion (grey-sparse bar) and FDCA yield (red-filled bar).

Regarding similar physical and chemical characteristics of R-V_2O_5 and V_2O_5 catalysts, discussed in the above section, HMF conversion was approximately 35-39%. Both R-V_2O_5 and V_2O_5 catalyst gave selectivity toward FDCA products 8-9%, and the yield of FDCA production was 5-7%. Catalytic oxidation performances of vanadium oxide doped on activated carbon were reported by Antonyraj and co-workers [21]. The V_2O_5/AC catalysts were tested under 100°C, methyl isobutyl ketone solvent (MIBK) 20 ml and with oxygen pressure 2.8 bar with catalyst loading 200 mg, the catalyst gave the highest conversion at 95.2%, and it was selective to DFF 96.4%, partly selective to FFCA only 3.6% and other by-products were absence. Vanadium oxide coated on hydrotalcite or alumina exhibited low HMF conversion 2.4-6.5% [21]. Vanadium oxide supported on acidic supports such as H-beta was tested under atmospheric pressure at 100°C with oxygen, and HMF conversion was 50%, and it gave DFF selectivity 45% [22] and testing condition was reported in Table 2. The oxidation of HMF was selective to DFF 50% over vanadyl phosphate [23]. The comparison of catalysts composed of vanadium with palladium doped on vanadium oxide was shown in Table 1. Unfortunately, all previous researches and our catalysts were carried out at different conditions. The present work exhibits the influence of noble metal palladium that can facilitate oxidation of HMF to FDCA, while vanadium oxide dominates oxidation of HMF to DFF. It was notable that the catalysts consisting of vanadium were remarkable on HMF oxidation to DFF. The influence of the redox mechanism discovered by Junfang Nie and co-authors [11]. The reduction of V^{5+} to V^{4+} could facilitate oxidation and dehydration of HMF convert to DFF at hydroxymethyl (R-OH) site, but the step of further oxidation is plausibly prolonged so that the reaction was rarely selective to FDCA.
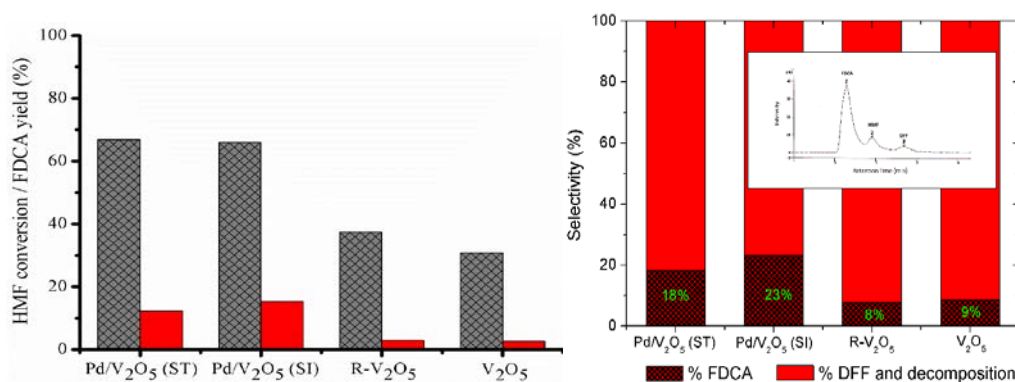

Figure 5. (Left) Catalytic activity test for four different catalysts: HMF conversion (grey-sparse bar) and FDCA yield (red-filled bar) (Right) Selectivity of four different catalysts toward FDCA and DFF and decomposition

Table 2. Selective Oxidation of HMF in the Catalysts Composed of Vanadium Oxide Compared to Present Work

Catalyst	Condition	% HMF Conversion	% Selectivity					Ref.
			FDCA	HMFCA	FFCA	DFF	Others	
V_2O_5/AC	100°C, 2.8 bar, O_2, 240 min (200 mg HMF, V/HMF molar ratio = 10, 20 ml MIBK	95.2	-	-	3.6	96.4	-	[21]
V_2O_5/H-beta	125°C, 10 bar, O_2, 180 min (100 mg HMF, 100 mg cat., 5 ml DMSO	84.0	-	-	-	98	2	[22]
$VOPO_4.2H_2O$	80°C, 1 bar, O_2, 360 min, 12 mmol HMF, 600 mg, 30 ml MIBK	98.0	-	-	-	50	50	[23]
Pd/V_2O_5(ST)	80°C, 1 bar, TBHP:HMF = 9:1, 24 h, 3 mmol HMF, 300 mg, 30 ml Acetonitrile	65.0	18	-	-	82		Present work
Pd/V_2O_5(SI)	80°C, 1 bar, TBHP:HMF = 9:1, 24 h, 3 mmol HMF, 300 mg, 30 ml Acetonitrile	65.0	23	-	-	77		Present work

Others: such as AMF: 5- acetoxymethyl-2-furaldehyde, OBMF: 5,5'-[oxybis(- methylene)]-bis-2-furaldehyde LA: Levulinic acid

The incorporation of 1 wt.% Pd NPs into V_2O_5 can increase HMF conversion from 20% to 65% as well as FDCA yields were approximately twofold increased. The Pd nanoparticles incorporated in V_2O_5 were more active than the bare V_2O_5 and reduced V_2O_5. It is because of the synergetic effect between Pd nanoparticles and V_2O_5. Nobel metals play an essential role in the high oxidation activity of HMF [5]. The FDCA yield percentage over Pd/V_2O_5 prepared from two different processes slightly differed; it is possible due to PdO impurity that exists in Pd/V_2O_5 derived by ST process. The PdO impurity can suppress the activity of the oxidation, and it is not comparable to palladium metal. FDCA yield was 12-15%. Besides FDCA, DFF intermediate was found. Figure 5 (right) exhibited product selectivity to FDCA, DFF, and decomposition of HMF. Most of HMF were decomposed, possibly due to the drastic oxidizing agent used (TBHP) and operating temperature. The HMF conversion was generally improved when increasing the reaction

temperature [21]; however, most of them were decomposed, leading to low product selectivity. Catalysts differed in chemical compositions, and surface chemistry needs appropriate conditions for selective oxidation such as temperature, base content, and solvents.

Conclusions

To summarize, Pd NPs incorporated in V_2O_5 catalysts were prepared by facile colloid-chemical reduction and immobilization methods. The sequence of reduction using $NaBH_4$ solution does not impact on physical and chemical characteristics of V_2O_5, but it does on Pd NPs. Palladium oxide was formed during ST process, namely as PdO impurity, while the Pd^0 NPs were completely immobilized to V_2O_5 during SI process because of no trace of Pd^{2+} signal in UV-visible spectrophotometry. The Pd/V_2O_5 catalysts prepared from these two different processes differed slightly in HMF conversion and FDCA yield because of the PdO impurity. The absolute Pd NPs loaded on V_2O_5 catalysts gave slightly superior FDCA yield for the oxidation. Besides that, the synergic effect of Pd NPs and V_2O_5 on the oxidation to FDCA and DFF should be noted.

Acknowledgments

References

[1] H. Kobayashi, and A. Fukuoka, "Synthesis and utilization of sugar compounds derived from lignocellulosic biomass," *Green Chemistry*, Vol. 15, No. 7, pp. 1740-1763, 2013.

[2] T. Werpy, and G. Petersen, *Top Value Added Chemicals from Biomass* [online]. Available: https://www.nrel.gov/docs/fy04osti/35523.pdf [Accessed: March 2019]

[3] A.B. Gawade, A.V. Nakhate, and G.D. Yadav, "Selective synthesis of 2, 5-furandicarboxylic acid by oxidation of 5-hydroxymethylfurfural over $MnFe_2O_4$ catalyst," *Catalysis Today*, Vol. 309, pp. 119-125, 2018.

[4] T.M. Research, "*2,5 Furandicarboxylic Acid (FDCA) Market: Snapshot*" 2018 [online] Available:https://www.transparencymarketresearch.com/furandicarboxylic-acid-arket.html [Accessed: June 2018]

[5] T. Gao, T. Gao, W. Fang, and Q. Cao, "Base-free aerobic oxidation of 5-hydroxymethylfurfural to 2,5-furandicarboxylic acid in water by hydrotalcite-activated carbon composite supported gold catalyst," *Molecular Catalysis*, Vol. 439, pp. 171-179, 2017.

[6] Y.Y. Gorbanev, S.K. Klitgaard, J.M. Woodley, C.H. Christensen, and A. Riisager, "Gold-catalyzed aerobic oxidation of 5-hydroxymethylfurfural in water at ambient temperature," *Chemsuschem*, Vol. 2, No. 7, pp. 672-675, 2009.

[7] S. Siankevich, G. Savoglidis, Z. Fei, G. Laurenczy, D.T.L. Alexander, N. Yan, and P.J. Dyso, "A novel platinum nanocatalyst for the oxidation of 5-Hydroxymethylfurfural into 2,5-Furandicarboxylic acid under mild conditions," *Journal of Catalysis*, Vol. 315, pp. 67-74, 2014.

[8] B. Zou, X.S. Chen, J.J. Xia, and C.S. Zhou, "Alkaline ionic liquid modified Pd/C catalyst as an efficient catalyst for oxidation of 5-hydroxymethylfurfural," *Journal of Chemistry*, Vol. 2018, No. 2018743, pp.1-9, 2018.

[9] L.F. Zheng, J.Q. Zhao, Z.X. Du, B.N. Zong, and H.C. Liu, "Efficient aerobic oxidation of 5-hydroxymethylfurfural to 2,5-furandicarboxylic acid on Ru/C catalysts," *Science China-Chemistry*, Vol. 60, No. 7, pp. 950-957, 2017.

[10] N.T. Le, P. Lakshmanan, K. Cho, Y. Han, and H. Kim, "Selective oxidation of 5-hydroxymethyl-2-furfural into 2,5-diformylfuran over VO^{2+} and Cu^{2+} ions immobilized on sulfonated carbon catalysts," *Applied Catalysis A: General*, Vol. 464-465, pp. 305-312, 2013.

[11] J. Nie, and H. Liu, "Aerobic oxidation of 5-hydroxymethylfurfural to 2,5-diformylfuran on supported vanadium oxide catalysts: Structural effect and reaction mechanism," *Pure and Applied Chemistry*, No. 84, p. 765, 2011.

[12] C. Moreau, R. Durand, C. Pourcheron, and D. Tichit, "Selective oxidation of 5-hydroxymethylfurfural to 2,5-furan-dicarboxaldehyde in the presence of titania supported vanadia catalysts," *Studies in Surface Science and Catalysis*, Vol. 108, pp. 399-406, 1997.

[13] Y.N. Zhao, W.W. Liang, Y.D. Li, and L. Lefferts, "Effect of chlorine on performance of Pd catalysts prepared via colloidal immobilization," *Catalysis Today*, Vol. 297, pp. 308-315, 2017.

[14] L. Shao, K. Wu, X. Lin, M. Shuinn, R. Ma, D. Wang, N. Long, Y. Ren, and J. Shun, "Sol-gel preparation of V_2O_5 sheets and their lithium storage behaviors studied by electrochemical and in-situ X-ray diffraction techniques," *Ceramics International*, Vol. 40, No. 4, pp. 6115-6125, 2014.

[15] T. Kumari, R. Gopal, A. Goyal, and J. Joshi, "Sol-gel synthesis of Pd@PdO core-shell nanoparticles and effect of precursor chemistry on their structural and optical properties," *Journal of Inorganic and Organometallic Polymers and Materials*, Vol. 29, No. 2, pp. 316-325, 2019.

[16] D. Jose, and B.R. Jagirdar, "Synthesis and characterization of Pd(0), PdS, and Pd@PdO core-shell nanoparticles by solventless thermolysis of a Pd-thiolate cluster," *Journal of Solid State Chemistry*, Vol. 183, No. 9, pp. 2059-2067, 2010.

[17] W.E. Mahmoud, and A.A. Al-Ghamdi, "The influence of vanadium pentoxide on the structure and dielectric properties of poly (vinyl alcohol)," *Polymer International*, Vol. 59, No. 9, pp. 1282-1288, 2010.

[18] R.S. De Oliveira, W.A. Alves, and E.A. Ponzio, "Spectroelectrochemical study of the hybrid between vanadium oxide and carboxybenzylviologen for application in electrochromic electrodes," *ECS Transactions*, Vol. 43, No. 1, pp. 363-369, 2012.

[19] N.H. Choi, S.-K. Kwon, and H. Kim, "Analysis of the oxidation of the V(II) by dissolved oxygen using UV-visible spectrophotometry in a vanadium redox flow battery," *Journal of The Electrochemical Society*, Vol. 160, No. 6, pp. A973-A979, 2013.

[20] N. Basavegowda, K. Mishra, and Y.R. Lee, "Ultrasonic-assisted green synthesis of palladium nanoparticles and their nanocatalytic application in multicomponent reaction," *New Journal of Chemistry*, Vol. 39, No. 2, pp. 972-977, 2015.

[21] C.A. Antonyraj, B. Kim, Y. Kim, S. Shin, K.Y. Lee, I. Kim, and J.K. Cho, "Heterogeneous selective oxidation of 5-hydroxymethyl-2-furfural (HMF) into 2,5-diformylfuran catalyzed by vanadium supported activated carbon in MIBK, extracting solvent for HMF," *Catalysis Communications*, Vol. 57, pp. 64-68, 2014.

[22] I. Sdaba, Y.Y. Gorbanev, S. Kegnæs, S.S. Reddy Putluru, R.W. Berg, and A. Riisager, "Catalytic performance of zeolite-supported vanadia in the aerobic oxidation of 5-hydroxymethylfurfural to 2,5- diformylfuran," *ChemCatChem*, Vol. 5, pp.284-293, 2013.

[23] C. Carlini, P. Patrono, A.M. Raspolli Galletti, G. Sbrana, and V. Zima, "Selective oxidation of 5-hydroxymethyl-2-furaldehyde to furan-2,5-dicarboxaldehyde by catalytic systems based on vanadyl phosphate," *Applied Catalysis A: General*, Vol. 289, pp.197-204, 2005.